4344–4353 *Nucleic Acids Research, 2018, Vol. 46, No. 9* *Published online 14 April 2018*
doi: 10.1093/nar/gky253

Dehydrated DNA in B-form: ionic liquids in rescue

Debostuti Ghoshdastidar and Sanjib Senapati*

Department of Biotechnology, BJM School of Biosciences, Indian Institute of Technology Madras, Chennai 600036, India

Received September 27, 2017; Revised March 03, 2018; Editorial Decision March 05, 2018; Accepted April 10, 2018

ABSTRACT

The functional B-conformation of DNA succumbs to the A-form at low water activity. Methods for room temperature DNA storage that rely upon 'anhydrobiosis', thus, often encounter the loss of DNA activity due to the B→A-DNA transition. Here, we show that ionic liquids, an emerging class of green solvents, can induce conformational transitions in DNA and even rescue the dehydrated DNA in the functional B-form. CD spectroscopic analyses not only reveal rapid transition of A-DNA in 78% ethanol medium to B-conformation in presence of ILs, but also the high resistance of IL-bound B-form to transit to A-DNA under dehydration. Molecular dynamics simulations show the unique ability of ILs to disrupt Na^+ ion condensation and form 'IL spine' in DNA minor groove to drive the A→B transition. Implications of these findings range from the plausible use of ILs as novel anhydrobiotic DNA storage medium to a switch for modulating DNA conformational transitions.

INTRODUCTION

DNA, by virtue of its attributes as a biological information carrier, is witnessing expanded applications into the fields of therodiagnostics (1,2), nanotechnology (3,4), digital information storage and beyond (5). The long-term structural stability of DNA is integral to all these applications. As DNA is vulnerable to hydrolytic and oxidative damage in aqueous solutions (6–9), ultralow temperatures are used for long-term storage of DNA. However, not only is refrigeration limited to small number of samples but repeated freeze-thaw of frozen samples can also cause structural damage to the DNA. As a result, techniques employing room-temperature storage of DNA is rapidly gaining popularity (8–10). Following nature's lead, most room-temperature storage methods employ the strategy of 'anhydrobiosis' or storage under a state of extreme dehydration (9,10). However, use of artificial agents to induce dehydration severely perturbs the DNA conformation, as water is essential for stabilizing the physiological B-form of double helical DNA. Several reports have shown that B-DNA succumbs to A-form upon dehydration down to a water activity (a_w) of 81% r.h. (11,12). Further dehydration can even lead to denaturation of natural DNA. Reports have also suggested that dehydrated DNA is more sensitive to damage by high temperature and UV radiation (9).

In recent years, a unique class of organic salts that are majorly liquid at room temperature (RT) and commonly known as ionic liquids (ILs) has gained increasing popularity as solvents for biomolecular solvation and stability (13–16). A pioneering work by Macfarlane and coworkers showed that ILs can maintain the chemical and structural stability of B-DNA at RT for long periods (15). Through a detailed investigation employing molecular dynamics (MD) simulations and spectroscopic experiments, we have shown that site-specific interaction of IL cations with DNA was the cause for such long-term conformational stability of DNA in ILs (16). Our study also suggested significant destabilization of the DNA solvation shell induced by IL cations. Since anhydrobiotic methods are the most conventional and effective ways to preserve DNA at RT, and since ILs destabilized the DNA solvation shell while maintaining the B-conformation, it would be worth investigating if the dehydrated A-form of DNA can be rescued to the physiological B-form by the addition of ILs. If successful, this could mark the advent of a superior next generation DNA storage technique for applications that require native DNA B-conformation to be preserved for long periods.

Hence, in this work we explore the conformational preferences of dehydrated DNA in the presence of ILs, and attempt to understand the underlying mechanism of conformational transitions in DNA, if any. To emulate the dehydrated condition, we selected the conventional ethanol/water mixture (>78% vol/vol ethanol/water). The low water activity (a_w) of this solvent medium ($a_w \leq 74.4\%$) is known to induce B-DNA to undergo a spontaneous conformational transition to the A-form (11,12,17). The B-conformation can be restored upon addition of water up to $a_w \geq 80\%$ r.h., which restores the DNA hydration shell that is known to be critical in maintaining the B-form (12,17). The indispensable role of water in inducing this classical hydration-mediated transition has been established by several experimental (12,17–19) and simulation studies (20–23). It would therefore be of tremendous fundamental and practical significance to study if ILs could bring about a

*To whom correspondence should be addressed. Tel: +91 44 22574122; Fax: +91 44 22574102; Email: sanjibs@iitm.ac.in

similar A→B transition of DNA without the aid of hydration, in other words obtain the dehydrated DNA in B-form.

MATERIALS AND METHODS

DNA samples

DNA from Salmon testes (*Oncerhynchus keta*) and all ILs were obtained from Sigma-Aldrich. DNA was sonicated down to 500 bp using a probe sonicator, precipitated with ethanol and re-constituted in water at a stock concentration of 100 μg/ml. All experiments were carried out in unbuffered solutions.

Preparation of A-DNA

The A-form of DNA was prepared as described earlier (11,12,17). Briefly, sonicated DNA was re-suspended in water at a stock concentration of 100 μg/ml and the NaCl concentration was adjusted to 300 μM. Step by step addition of ethanol with constant stirring generated the A-form, indicated by a molar dichroism of $\Delta\varepsilon = 8$–9 at the CD maximum (268 nm). This solution form of A-DNA was used as the starting point for carrying out the CD experiments to study A→B-DNA transition. CD spectra were recorded at 25°C.

IL-induced A→B-DNA transition

Calculated quantities of stock IL/water solutions were added to the A-DNA solution and the CD spectra were recorded. For all ILs, the complete transition to B-DNA was attained within an IL concentration of 1.5 mM. During the course of IL addition, the ethanol concentration was maintained within 76.8% to ensure that the observed transition was mediated by ILs and not by a change in the water activity of the solution.

Back-extraction of DNA from DNA-IL solutions

To prepare DNA-IL solutions, measured quantities of Salmon testes DNA were suspended in IL/water binary mixtures containing 20wt% [bmim][Ac] or [chol][Ac] ILs to obtain a final DNA concentration of 2 mg/ml. DNA concentrations were determined using an extinction coefficient of 6600 M^{-1} cm^{-1} at 260 nm and expressed in terms of base molarity. Back-extraction of DNA fraction from these IL/water binary mixtures was carried out by precipitating with ice-cold ethanol in the presence of 3M sodium acetate salt. The mixture was centrifuged and the recovered DNA pellet was re-suspended in 1× TE buffer. Ethanol precipitation was carried out up to three times for each solution to attempt complete removal of IL from the DNA. Electrophoresis of regenerated DNA was carried out on 2% agarose gels.

MD simulations

MD simulation set up and performance were carried out using the Amber package (24). The well characterized DD dodecamer was used as the model to study the conformational transition in double helical DNA. The canonical A- and B-forms of the dodecamer used as starting structures for all simulations were generated using the nucleic acid builder (NAB) utility within the Amber14 module (24). Interaction potentials were defined within the OPLS-AA/AMBER framework (25). To begin with, we performed three control simulations of (i) A-DNA in 85% ethanol (system 7 in Supplementary Table S1), (ii) A-DNA in water (system 8 in Supplementary Table S1) and (iii) B-DNA in water (system 9 in Supplementary Table S1). The A-conformer is typically simulated in an ∼85% ethanol/water mixture, since a lower or higher a_w appears to perturb the helicoidal geometry of A-DNA (20). The control systems were built and simulated following the well-established protocol described by Cheatham *et al.* (20) as further detailed in SI Methods. For simulating the IL-induced A→B-DNA transition, average structure of the simulated A-DNA in 85% ethanol (system 7) along with its condensed cloud of Na-counterions was used as the starting structure. This was done to emulate the experimental protocol, wherein ILs were titrated into the DNA/ethanol solution that already contained NaCl. Twenty two [bmim][Ac] or [chol][Ac] ILs were randomly placed around the DNA, with at least 10 Å distance from the phosphate backbone. Subsequently, each system was thoroughly equilibrated. To enable volume variation, simulations were performed in an NPT ensemble using the Berendsen thermostat and barostat. The calculation of long-range Coulombic forces was performed employing the full Ewald summation technique. The real space part of the Ewald sum and Lennard-Jones interactions were cut off at 15 Å. SHAKE was used to constrain bond lengths between heavy atoms and hydrogens. Following equilibration, an unrestrained production run of 200 ns was performed for each DNA-IL system. All analyses were carried out using in-house codes and the cpptraj module in Amber 14 (24).

RESULTS AND DISCUSSION

Dehydrated DNA transits to B-form under the influence of ILs

Two of the most physiologically relevant conformers of DNA, the A- and B-forms, exist under conditions of low and high hydration, respectively (12,17,18). Different hydration levels can be attained *in vitro* by changing the water activity (a_w) of the aqueous solvent medium with the addition of ethanol, and the resulting conformational transitions in DNA are monitored using circular dichroism (CD) spectroscopy. The characteristic CD spectrum of B-DNA in aqueous solution comprises of a positive and a negative peak of equal intensities at 278 and 245 nm respectively, with a cross-over at 260 nm (Supplementary Figure S1, dashed line). As shown in Supplementary Figure S1, upon addition of up to 78% ethanol (a_w of 74.4% r.h.), B-DNA transited to the A-form as indicated by characteristic changes in all the CD signals. The positive CD signal at 278 nm intensified and underwent a blue shift, the negative peak at 245 nm almost disappeared, while a negative peak at 211 nm became prominent.

To investigate if ILs can play any role in the conformational transitions of DNA, we added a series of high-to-moderately biocompatible ILs—[1-ethyl-3-methyl

imidazolium][acetate] ([emim][Ac]), [1-butyl-3-methyl imidazolium][acetate] ([bmim][Ac]), [cholinium][acetate] ([chol][Ac]), [1-ethyl-3-methyl imidazolium][lactate] ([emim][Lac]) and [cholinium][lactate] ([chol][Lac])—into the dehydrated environment of 78% ethanol/water containing the A-form of DNA. Interestingly, A-DNA showed a clear transition to the B-form with the progressive addition of ILs, despite the dehydrated medium as shown in Figure 1. The transition was completed with the addition of a maximum 1.5 mM concentration of all ILs studied, beyond which overlapping peaks characterizing the B-form were obtained. This is remarkable, because the water activity of the final solution containing B-DNA corresponds to 75.3% r.h. (76.8% ethanol), which is classically known to harbour the A-form of DNA (Supplementary Figure S1) (11,12). Since DNA typically exists in A-conformation in dehydrated medium, it is of immense fundamental and practical importance to understand how ILs can cause an A→B-DNA transition under dehydration. Hence, we resorted to all-atom MD simulations, which have been proven to be very effective in exploring the conformational transitions in DNA (20–23).

Mechanism of IL-induced A→B-DNA transition under dehydration

To study conformational dynamics in DNA using MD simulations, the Dickerson-Drew (DD) dodecamer [$(CGCGAATTCGCG)_2$] is commonly used as a model sequence since it does not show a bias towards either A- or B-conformer. Moreover, the DD dodecamer is the minimal model available that possesses a complete helical turn, which is key to studying transitions in DNA helical parameters during conformational change (Supplementary Figure S2). The A-conformer is typically simulated in an ∼85% ethanol/water mixture, since a lower or higher a_w appears to perturb the helicoidal geometry of A-DNA (26). Hence, to elucidate the mechanism of A→B transition of DNA caused by ILs under dehydration, we simulated the A-conformer of the dodecamer in 85% ethanol/water mixture in the presence of representative ILs—[bmim][Ac] and [chol][Ac]. Additionally, three control simulations were performed: (i) A-DNA in 85% ethanol/water mixture, (ii) A-DNA in water and (iii) B-DNA in water, in the absence of ILs. The details of the simulated systems are tabulated in Supplementary Table S1. Conformational transitions of the dodecamer along the simulation trajectory were monitored by calculating its root mean square deviation (RMSD) from the B-DNA crystal structure. As summarized in Supplementary Figure S3, the A-conformer remained stable in 85% ethanol/water mixture indicated by its persistently high RMSD from the crystal B-conformer, while it promptly transited to the B-form in water indicated by a rapid decrease in RMSD (Supplementary Figure S3 inset). More interestingly, in the presence of ILs, A-DNA displayed the unusual transition to the B-form even in the dehydrating ethanol/water medium, in agreement with our CD spectroscopic data. In the presence of [bmim][Ac], the A-conformer showed strong perturbations early on in the simulation up to 60 ns, beyond which the RMSD steadily decreased before stabilizing within 2.0 Å of the B-DNA geometry at ∼100 ns. The structural transition in the presence of [chol][Ac] began early at ∼25 ns and appeared to be more abrupt, with the RMSD rapidly converging close to the B-conformation at ∼35 ns. After the transition was completed, DNA maintained a stable B-conformation for the remaining simulation period in both ILs.

IL cations disrupt Na^+ ion condensation at the major groove of A-DNA. The conformational preference of DNA for the A-form at low water activity can be ascribed to its architecture. Being more compact, the major groove of A-DNA harbours dense negative charge, which becomes a hub for increased condensation of counter-ions promoted by the low-dielectric ethanol medium (26,27). These Na-counterions bridge between phosphate oxygens on complementary strands of A-DNA either directly or through water molecules, thereby lowering inter-phosphate repulsions and electrostatically stabilizing the A-form (21). In presence of ILs, this condensation of counterions is greatly affected (Figure 2). As shown in Figure 2A, at the onset of the simulation a condensed cloud of Na^+ counterions was present near the major groove edge of the A-form. The condensed Na^+ ions in the major groove formed up to five cross-strand bridges in the control A-DNA simulation (Figure 2B). In the presence of ILs, the counter-ion condensation at the major groove was impaired (Figure 2C) leading to a gradual depletion in the number of Na-bridges (Figure 2D). Instead, a significant number of IL cations were found to localize near the B-DNA backbone in these water-deficient systems, as shown in Figure 2D (green rings). Notably, this distribution of IL cations mimics the so-called 'cone-of-hydration' - the shell of water molecules solvating the B-DNA backbone in water (21). In our study, since the A→B transition occurred under conditions of extreme dehydration, formation of a hydration cone was not possible, and thus the IL cations came in rescue to stabilize the B-DNA backbone.

Ionic liquids bind to the DNA minor groove. Apart from interacting with the phosphate backbone, IL cations also interacted very strongly with the DNA minor groove, as exemplified by two sharp peaks in its radial distributions around DNA (Supplementary Figure S4). A 3D view of IL cation–minor groove binding presented in Figure 3A and B depicts randomly distributed water molecules in the minor groove of A-DNA being replaced by an ordered network of IL cations upon transiting to B-DNA. A closer look revealed that these IL cations approached the minor groove at different junctures *en route* transition and localized in the groove for extended periods of time (Figure 3C). Figure 3D presents snapshots of the binding events of three such [bmim] cations designated as IL-1, IL-2 and IL-3 in the chronological order of their intrusion into the minor groove. Interestingly, as shown in Figure 3C and D, with the approach of each IL close to the DNA groove, the A-conformer is significantly perturbed. This strong interplay between minor groove binding of IL cations and the conformational transition of A-DNA to B-form is also evident from Figure 3D and E, which show a gradual decay in RMSD values at the time of IL intrusions followed by a

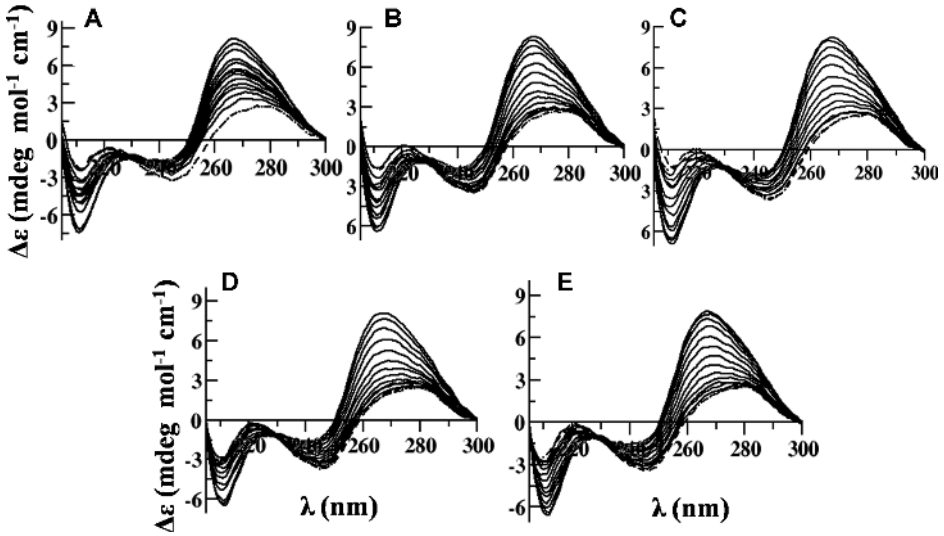

Figure 1. Ionic liquids induce an unusual A→B-DNA transition in a dehydrating 78% ethanol/water mixture. The typical A-DNA (topmost curve in each graph) transits to the B-form (indicated by dashed line) induced by a range of ILs: (**A**) [bmim][Ac], (**B**) [chol][Ac], (**C**) [emim][Ac], (**D**) [chol][Lac], (**E**) [emim][Lac]. [DNA] = 3×10^{-4} M **bps**, [NaCl] = 3×10^{-4} M, [IL] ($\times 10^{-4}$ M): 0.0, 0.5, 1.0, 2.0, 3.0, 4.0, 5.0, 6.0, 7.0, 8.0, 9.0, 10.0, 11.0 and 15.0 (from top to bottom in each plot). The CD spectra were normalized to account for the change in DNA concentration with increasing addition of IL solutions.

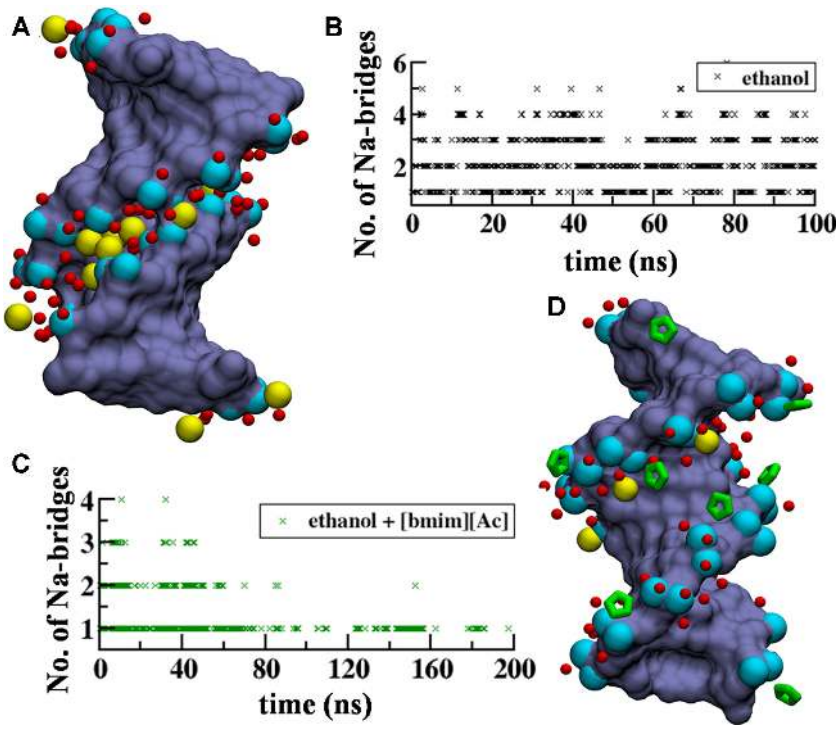

Figure 2. Counter-ion condensation is impaired *en route* A → B transition of DNA. (**A**) Na-counter-ions (yellow) condense near the phosphate groups (cyan) of A-DNA to form (**B**) cross-strand Na-bridges in the control simulation of A-DNA in 85% ethanol/water mixture. During IL-induced transition of A-DNA to the B-form (**C**) the number of Na-bridges deplete as ion-condensation is disrupted and (**D**) replaced by IL cations (green rings). Water oxygens are shown in red. Only the imidazolium ring of the IL cation is shown for clarity. A cross-strand Na-bridge was defined as a Na^+ that was simultaneously found within ~3.5 Å distance between two cross strand phosphate oxygens.

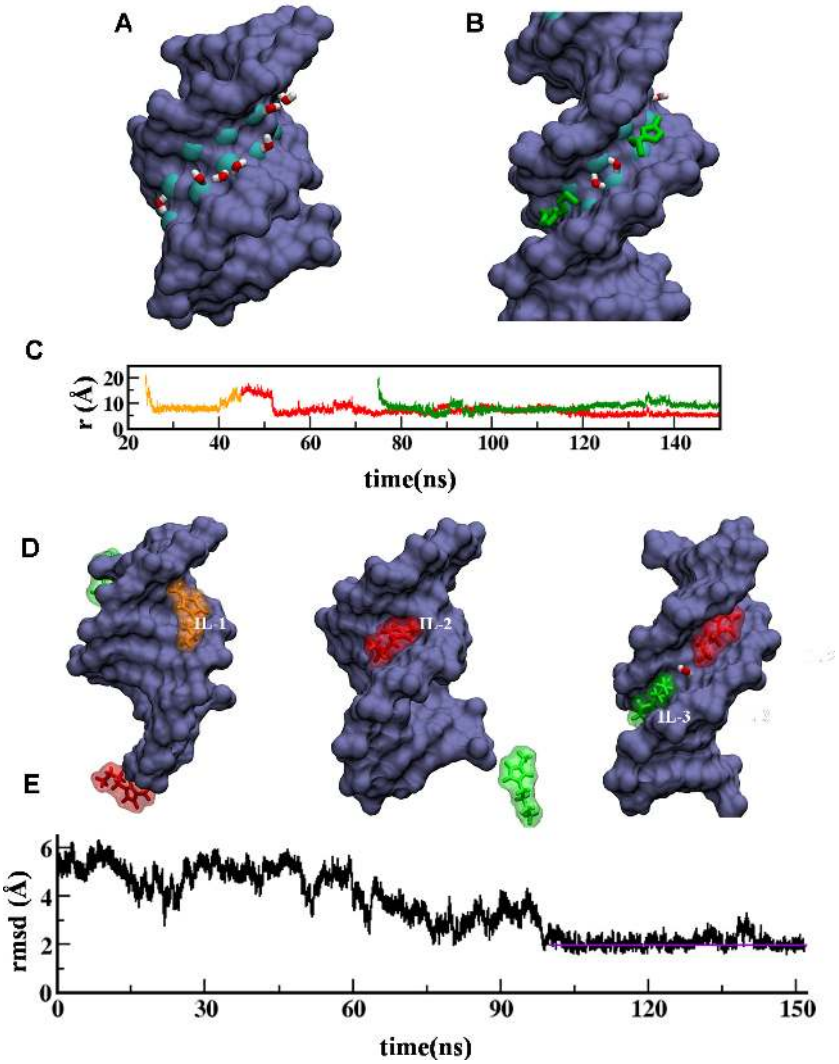

Figure 3. Key events occuring in the minor groove during the course of IL-induced A→B-DNA transition. (**A**) A disordered hydration network in A-DNA is replaced by (**B**) an ordered $[bmim]^+$-water spine in B-DNA (IL cations, green; base atoms, cyan). (**C**) Intrusion of IL cations is represented as distance plots between ILs and the DNA minor groove as a function of time. (**D**) Snapshots of the IL-bound DNA are shown at time points 25, 70 and 100 ns for IL-1, IL-2 and IL-3, respectively, which persisted in the minor groove during the course of the transition. (**E**) IL-DNA binding events severely perturb the A-DNA structure causing strong fluctuations in RMSD until at ∼100 ns when IL-induced A→B-DNA transition completed and the RMSD converged within 2 Å of the B-DNA geometry.

plateau characterizing the appearance of a stable B-DNA conformation.

Conformational transitions in DNA are always accompanied by changes in several helicoidal parameters (20,23,28,29). Time evolution of various helicoidal parameters in Supplementary Figure S5 suggests that all the studied parameters fluctuated close to the A-DNA geometry up to ∼60 ns before steadily transiting towards their values in B-conformer. Such concerted global changes in the helicoidal parameters of DNA are known to be the manifestations of local changes occurring at each base pair step (29). Interestingly, analysis of individual step parameters revealed that the most vivid transitions occur at base pairs that serve as sites for IL binding. Figure 4 presents the time evolution of inclination (INC), *x*-displacement (XDP) and roll at base pair steps 5A:20T | 6A:19T and 7T:18A | 8T:17A where IL-2 and IL-3 were bound, respectively. Apart from a sharp departure at ∼20 ns, all three parameters of the base pair step 5A:20T | 6A:19T exhibited values close to the A-form up to ∼50 ns. The deviation at ∼20 ns can be attributed to the short intermittent interaction made by IL-1 with these base pairs. Beyond 50 ns the parameters deviated from their values in the A-conformer and approached very close to the B-form values at 60 ns. This corresponds well with the time of IL-2 binding to this base pair step (see Figure 3D). Similarly, binding of IL-3 at 7T:18A | 8T:17A causes a strong transition of this base pair step towards the B-conformation at ∼75 ns. Moreover, owing to the intrinsic cooperativity in the DNA structure, binding of IL-3 in the adjoining region has a stabilizing effect on the B-DNA geometry at 5A:20T | 6A:19T base pair step as well. However, it is noteworthy that the base pair step 7T:18A | 8T:17A itself exhibits a sharp transition to the B-form only after a while (at ∼100 ns). Following this event the entire dodecamer attains the B-

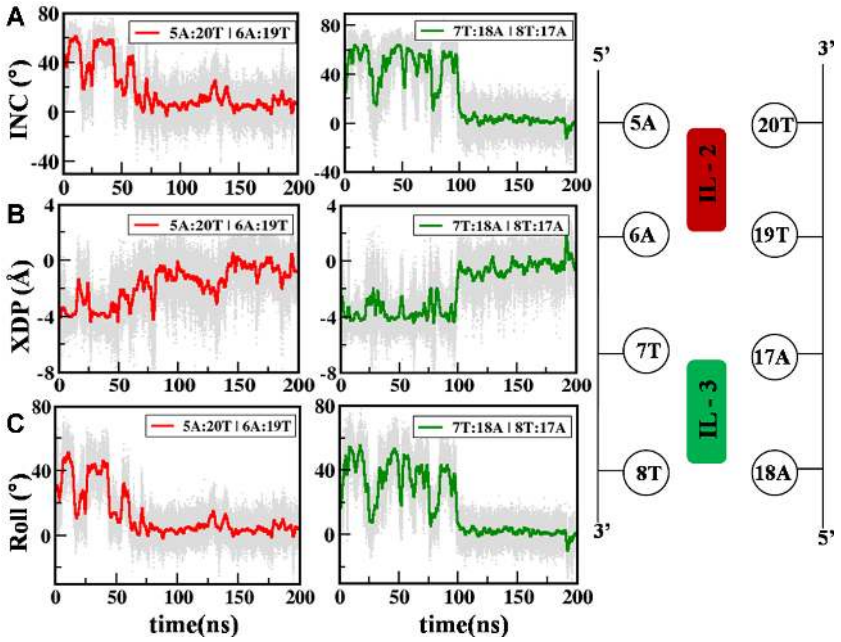

Figure 4. Time evolution of geometrical parameters (**A**) inclination (INC), (**B**) X-displacement (XDP) and (**C**) roll at base pair steps 5A:20T | 6A:19T (left panel) and 7T:18A | 8T:17A (right panel) during the course of IL-induced A→B-DNA transition in 85% ethanol/water mixture. The background distribution (gray) presents geometrical parameter data recorded every 2 ps during the simulation, while the projected distributions (red/green) are running averages calculated over 1000 ps windows. A schematic representation of the binding of IL-2 and IL-3 to the above base pair steps is shown for reference. Standard average values of geometrical parameters: A-DNA: INC = >20°, XDP = −5 Å, roll = >+12° and B-DNA: INC = 3.4°, XDP = −1 to 0 Å, roll = 0°.

DNA geometry (see Supplementary Figure S3), indicating that transition of the central AATT step could be essential to drive transition of the entire DNA to the B-form.

A recent study by Lavery *et al.* suggested that often simulations up to 300ns are required to obtain stable ion distributions around helical DNA (30). Hence, simulation of DNA dodecamer in the [bmim][Ac]/water/ethanol system was extended up to 400 ns. As shown above, during the transition period (80–120 ns), distributions of ions in DNA grooves and around the phosphate backbone were severely perturbed (Supplementary Figure S6). However, immediately after transition, the ion/solvent distribution re-equilibrated to attain a plateau, which was sustained until the end of the simulation. This confirmed that stable ion distribution was attained in our simulated systems. Slightly higher fluctuations in ion distribution in the major groove occur due to the wider space available for exchange of ions, unlike the constricted minor groove.

IL-water spine stabilizes B-DNA. The preferential transition of DNA to the B-conformer upon IL binding now needed a more mechanistic elucidation. Hence we probed the DNA–IL interactions in greater detail. The intruding [bmim] cations did not simply reside in the minor groove of the DNA dodecamer, but formed H-bonding interactions with the electronegative base atoms. As shown in Figure 5A, the acidic hydrogen of the cation imidazolium ring simultaneously formed H-bonds with adenine-N3 on one strand and thymine-O2/cytosine-O2 on the complementary strand at the minor groove. The IL-mediated H-bond bridges were better characterized by deducing the time evolution of their formation over the course of the A→B transition. As shown in Figure 5B, since its time of binding at the 5A:20T | 6A:19T step, IL-2 persistently bridged bases 6A and 20T till beyond the transition time. In a similar manner, IL-3 bound at base pair step 7T:18A | 8T:17A mediated a cross-strand bridge between bases 8T and 18A. Interestingly, the geometry and persistence of these cross-strand bridges posed a striking similarity to the water-mediated bridges constituting the spine of hydration in the control simulation of B-DNA in aqueous solutions (Supplementary Figure S7A). Notably, formation of the hydration spine is known to be critical in driving the A→B transition in aqueous solutions (31). The remarkable ability of the IL cation to mimic water in its interactions with the DNA minor groove causes a similar conformational transition of IL-bound base pairs even in the absence of sufficient water. The transition, however, was not yet fully complete. This is because the bulky [bmim] cations bound at the two AT steps excluded the central TT region of the AATT stretch from IL occupancy. Nonetheless, there was enough room for one water molecule to squeeze in between the two cations (Figure 5A). Further analysis revealed that the 7T-19T bridge was indeed formed by water (Figure 5C). Thus, an IL-water-IL spine spanning the entire AATT region promptly transited the DNA dodecamer to the B-conformation. It is important to note that the 'spine of IL cations' significantly differs from the 'spine of hydration' in that the former contains only a minor proportion of water. Replica simulations were carried out to validate the convergence of timescale and proposed mechanism of IL-induced A→B-DNA transition. The details of the replica simulations are summarized in Supplementary Table S1. As shown in Supplementary Figure S8,

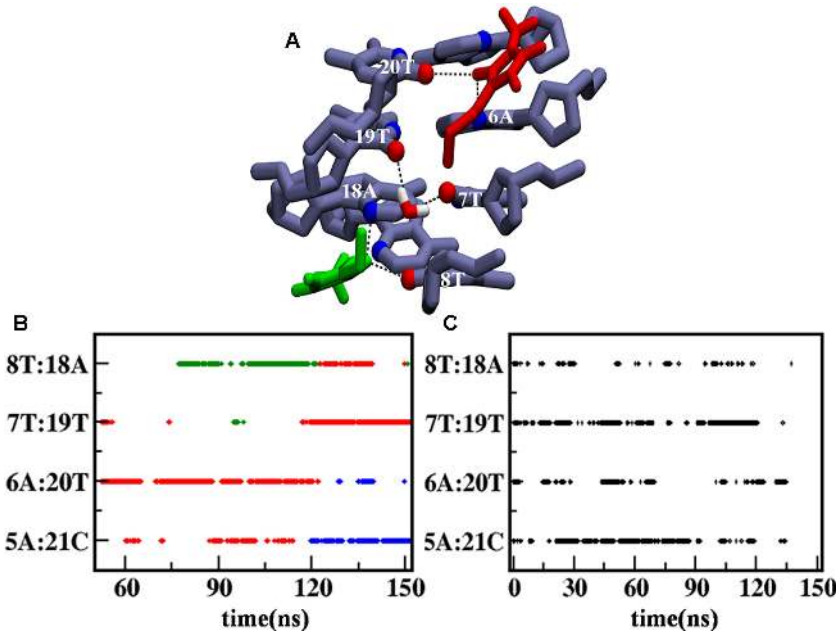

Figure 5. Spine of IL-water stabilizes B-DNA. (**A**) A [bmim]/water spine in the minor groove of B-DNA comprises of bifurcated H-bonds (dashed lines) formed by the acidic C1 carbon of the [bmim] cations (red and green) or O of water molecule with N3 and O2 atoms of the DNA bases. Persistence of the (**B**) [bmim] and (**C**) water constituents of the IL-water spine. The IL-water spine is dynamic indicated by the different ILs (red/green/blue) that constitute the spine during the transition period. To emphasize on the transition period, data beyond 150 ns are truncated.

the [bmim]-induced transition always occurs in ≤100 ns and this timescale remarkably coincided with the complete formation of the [bmim]-water spine in the DNA minor groove. This further reiterates that the IL-water spine brings about the A→B transition of DNA under conditions of severe dehydration.

Key role of AT in nucleating IL-induced DNA transition. An interesting fact that becomes evident from the above findings is that IL cations bind preferably at AT-rich regions of the DNA minor groove, which consequently serve as sites for nucleating the A→B transition (Figures 4 and 5). To investigate a plausible sequence-dependent nature of the IL-mediated A→B transition, we simulated two more dodecamers with sequences (i) 5′-CTTCCATGGAAG-3′ and (ii) 5′-CCCCCGCGGGGG-3′, denominated as AS1 and AS2, respectively. The first sequence contains an A-philic GC-rich core unlike the B-philic AATT segment of the DD dodecamer, while the second sequence completely lacks AT-base pairs. The A-form of the two duplexes were simulated in 85% ethanol/water mixture in the presence of [bmim][Ac]. As shown in Supplementary Figure S9, AS1 transited to the B-form in the presence of ILs even in the dehydrating ethanol medium, while AS2 failed to undergo a conformational change.

To understand the effect of DNA sequence on IL-induced A→B transition, the key events occurring during the simulation of AS1 and AS2 were captured. Initial perturbations of the AS1 A-DNA were caused by disruption of Na-bridges at the major groove and binding of IL-1 to a terminal AA step (Supplementary Figure S10A–C). Subsequently, IL-2 and IL-3 intruded into the minor groove of the dodecamer at different points of time (Supplementary Figure S10D), following which AS1 attained a stable B-form. Interestingly, all three ILs bound at AT base pairs in agreement with the preferential affinity of IL cations (Supplementary Figure S10D). Evidently, the course of events leading to the transition of AS1 matched well with our previous observations on the DD dodecamer, despite their distinct sequences. However, there was one notable difference in the nature of the spine formed in the minor groove of the two duplexes. Unlike the IL/water spine that aided in transition of the DD dodecamer (Figure 5), AS1 harboured a spine made solely of IL cations (Supplementary Figure S10E). This is because the predominance of GC base pairs at the central domain of the AS1 duplex prevented the formation of a stable water bridge at its minor groove (Supplementary Figure S11).

The AS2 dodecamer, on the other hand, primarily sampled the A-conformation during most of the simulation time. However, at least twice during the course of the simulation, its geometry showed strong fluctuations towards the B-form (at ∼60 and 100 ns in Supplementary Figure S9). As shown in Supplementary Figure S12, these structural perturbations were caused by disruption of Na-bridging at the major groove, similar to the DD and AS1 dodecamers. However, no IL cations made persistent interactions in the minor groove of AS2. As a result, although the A-form was perturbed, the B-form did was not stabilized and the DNA returned to its A-conformer.

Nature of IL cation dictates the promptness of A→B transition. When the [bmim] cation was replaced by [chol], transition of A-DNA to the B-form followed a similar mechanism—counter-ion condensation at the major groove of A-DNA was impaired and an IL/water spine was con-

stituted in the minor groove of B-DNA. However, the nature of the transition was quite distinct for the two ILs, with [chol][Ac] inducing a more abrupt A→B transition (Supplementary Figure S3). Similar to [bmim], several [chol] cations localized in the minor groove of DNA at different time points during the course of the transition (Supplementary Figure S13). The rapid transition induced by the latter can be attributed to the differential interaction made by the two cations with DNA. The positive charge on the [chol] head group is more localized compared to the imidazolium ring of [bmim], in which the charge is distributed over five different sites. As a consequence, [chol] cations experience a greater affinity for the negatively charged DNA backbone and grooves that plausibly brings about a more prompt A→B transition. Another noteworthy feature is that the water-assisted [chol]-spine formed at the minor groove contains more water than [bmim]-spine during most of the simulation period (compare last snaps of Supplementary Figure S13B and Figure 3D). However, it is only after the binding of IL-1 to 5A:20T | 6A:19T base pair step at ∼25 ns that these water persistently stay in the minor groove. The existence of more water in the minor groove of [chol]/DNA complex can be ascribed to two main reasons. Firstly, the small chain length of the choline moiety leaves more room for water occupancy. Secondly, the hydroxyl group of choline facilitates H-bonding interactions with water in the minor groove.

IL-bound B-DNA resists transition to the A form. The remarkable ability of ILs to restore the B-conformation of DNA elicits an interesting plausibility with significant potential applications—could ILs altogether prevent B-DNA from transiting to the A-form upon dehydration? To investigate this, we added our series of ILs to aqueous solutions of B-DNA, and subsequently subjected the IL-bound DNA to dehydration by gradual addition of ethanol. Quite surprisingly, B-DNA bound to [bmim][Ac] IL did not transit to the A-conformation even at 78% ethanol concentration. As shown in Figure 6A, the typical changes in CD bands that signify a B→A-DNA transition was not observed (compare with Supplementary Figure S1). Instead, a set of peaks of almost overlapping signal intensities corresponding to the B-DNA spectrum was obtained. This indicates that once bound to [bmim][Ac], the B-form is so stabilized that it resists transition. From our observations, the resistance of the IL-bound B-DNA to a conformational change can now be attributed to the IL-water spine persisting in the minor groove, which locks DNA in its B-conformation (Figure 3). Moreover, since water constitutes a very small proportion of the IL-water spine (Figures 3 and 5), dehydration imposed by addition of ethanol cannot disintegrate the spine or destabilize the B-conformation. Thus, binding of the [bmim] cation to the minor groove of A-DNA not only drives it to the B-form, IL-bound B-DNA also resists a conformational transition upon dehydration.

B-DNA bound to other ILs comprising of [chol] and [emim] cations exhibited similar, though slightly weaker, resistance to a conformational change to the A-form when subjected to dehydration. As shown in Figure 6B, with addition of up to 73% ethanol, choline-bound DNA maintained the B-conformation. Only upon further dehydration, conformation of the choline-bound B-DNA tends towards the A-form, although the increase in magnitude and the blue shift of the peak at 278 nm are clearly much lesser compared to the classical B→A transition (compare with Supplementary Figure S1). Irrespective of the type of IL cation or anion, similar resistance was exhibited by all IL-bound B-DNA (Supplementary Figure S14). The resistance to conformational transition posed by IL-bound B-DNA can be better comprehended by deducing the change in the B-form fraction ($[\theta]_B$) as a function of ethanol concentration. The CD spectrum was recorded at 270 nm for all ethanol concentrations and the B-form fraction was calculated as follows:

$$[\theta]_B = (\Delta\varepsilon - \Delta\varepsilon_A) / (\Delta\varepsilon_B - \Delta\varepsilon_A),$$

where $\Delta\varepsilon$ is CD_{270} at any given ethanol concentration and $\Delta\varepsilon_A$ and $\Delta\varepsilon_B$ are CD_{270} values for the A- and B-forms, respectively. As presented in Figure 6C, in the absence of ILs, B-DNA rapidly transited to the A-form with increasing addition of ethanol resulting in a classical sigmoidal curve depicting a cooperative transition. However, when bound to ILs, the resistance offered by the B-form to a conformational transition resulted in a plateaued curve up to high ethanol concentrations of ≥72%. In the absence of ILs, at least 50% of the DNA have already transited to the A-form at this ethanol concentration. Notably, $[\theta]_B$ for [bmim]-bound DNA could not be measured, as this DNA did not transit to A-form at all.

The greater effectiveness of [bmim] compared to the other ILs (compare Figure 6A and B) could be explained from our MD data. As shown in Supplementary Figure S15, the planar imidazolium ring of the [bmim] cation fits effectively into the minor groove pocket making greater number of contacts with the DNA base atoms. Conversely, the bulky $N(Me)_3$ headgroup of choline cation is sterically hindered from approaching the minor groove very closely. This is reflected in the free energy of binding values of the two ILs to B-DNA in 85% ethanol/water solution, –7.30 ± 1.43 kcal/mol for $[bmim]^+$ and –6.53 ± 0.44 kcal/mol for $[chol]^+$. Even though we do not have simulation data of DNA in [emim]-based IL, it is easy to conceive that the weak binding of [emim] in B-DNA minor groove is due to weaker van der Waals interaction of the ethyl side chain of [emim] compared to the long butyl chain of [bmim].

To affirm the greater binding strength of [bmim], we attempted to regenerate the free DNA from the respective IL-bound DNA fractions, and subsequently, tested the regenerated DNA using gel electrophoresis. As shown in Figure 6D, DNA recovered from [chol][Ac] solution moved as a distinct narrow band on agarose gel, while DNA regenerated from the [bmim]-bound fraction formed a broader band. The band trail observed for the latter can be ascribed to two reasons: (i) degradation of DNA or (ii) the presence of residual IL ions that hinder electrophoretic movement. Since the structural integrity of the regenerated DNA fractions was confirmed using CD spectroscopy (Supplementary Figure S16), the broader band plausibly resulted from a drag on the DNA passage through the gel caused by residual $[bmim]^+$ bound to DNA. Notably, both IL-bound DNA fractions were washed thoroughly and treated by identical protocols for the regeneration of free DNA. However, the

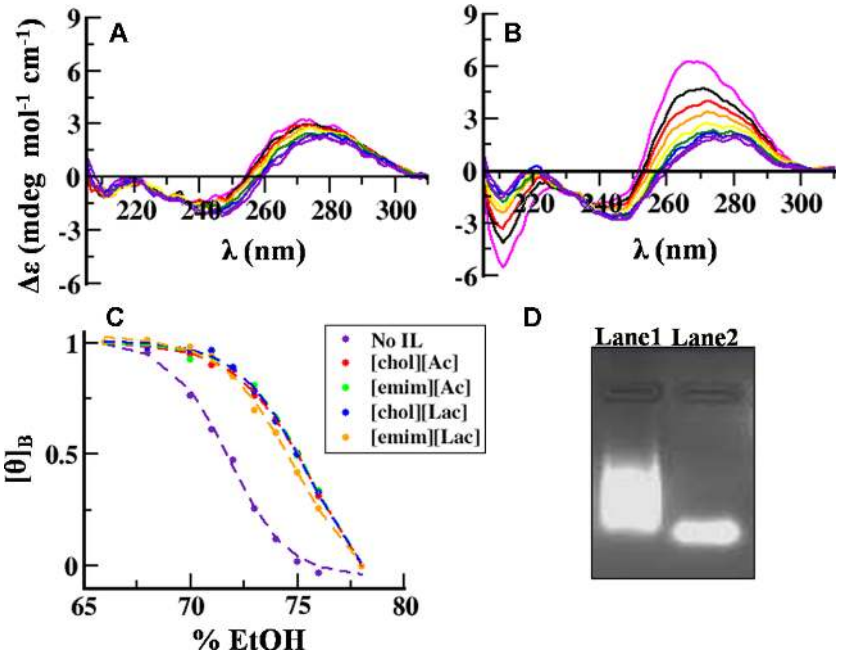

Figure 6. B-DNA bound to IL cations resist transition to the A-form even upon dehydration. (**A**) [bmim]-bound DNA offers the highest resistance by not transiting to the A-form at all. (**B**) Slightly weaker resistance is posed by B-DNA bound to [chol][Ac]. [DNA] = 3×10^{-4} M **bps**, [NaCl] = 3×10^{-4} M, [IL] = 3×10^{-4} M. Ethanol concentrations of 68, 70, 71, 72, 73, 74, 75, 76 and 78% are colour coded as VIBGYORBlackMagenta, respectively. The CD spectra were normalized to account for the change in DNA concentration with addition of ethanol. (**C**) Change in the fraction of DNA present in the B-form ($[\theta]_B$) as a function of added ethanol. (**D**) Gel electrophoresis of DNA extracted from DNA-IL solutions containing [bmim][Ac] (Lane 1) or [chol][Ac] (lane 2). The band trail in lane 1 indicates presence of residual [bmim] cations in the extracted DNA fraction.

strongly bound $[bmim]^+$ could not be completely removed from the DNA, unlike $[chol]^+$. This unequivocally proves that $[bmim]^+$ cations indeed bind with greater strength at the DNA groove compared to other ILs. The implications of this stronger binding manifest in better resistance of [bmim]-bound DNA to a conformational transition compared to [choline]-bound DNA.

CONCLUSIONS

It is classically known that the level of hydration is the most important determinant of the conformational state of DNA. The physiological B-conformation succumbs to A-form under conditions of dehydration. Here we show for the first time that ILs can induce conformational transitions in DNA, and even retain the B-form under a state of extreme dehydration. Results suggest that ILs accomplish this unusual phenomenon by a two-fold mechanism—destabilizing the A-form by disrupting counter-ion condensation and stabilizing the B-form by establishing an 'IL spine' in the minor groove. The nature and interactions of this 'IL spine' bear striking similarity with the classical 'spine of hydration' known to stabilize B-DNA in water. Results also suggest that ILs nucleate the A→B transition by its preferential binding at AT steps. Thus, while AT base pairs present in the DNA sequence can serve as sites for initiating a conformational change, sequences lacking AT regions fail to undergo the transition. Moreover, the type of IL cation dictates the promptness of A→B transition and is also a key determinant of the extent of transitional resistance that B-DNA would experience in dehydrated conditions. The implications of these findings could mark the leap ahead in the applications of ILs in DNA technology. For example, ILs can now be integrated into an 'anhydrobiotic' DNA storage media as a stabilizer against conformational transition due to dehydration. But even more remarkable will be the plausible use of ILs as a conformational switch for DNA through careful selection of the IL cationic counterpart and the DNA sequences.

SUPPLEMENTARY DATA

Supplementary Data are available at NAR Online.

ACKNOWLEDGEMENTS

The facilities provided by DST-FIST, Govt. of India and Computer Centre, IIT Madras are greatly acknowledged. DG thanks Md. Homaidur Rahman and Rajani K. for help with experiments.

FUNDING

SERB, Govt. of India [EMR/2016/000707]. Funding for open access charge: DST, Govt. of India [EMR/2016/000707].
Conflict of interest statement. None declared.

REFERENCES

1. Patil,S.D., Rhodes,D.G. and Burgess,D.J. (2005) DNA-based therapeutics and DNA delivery systems: a comprehensive review. *AAPS J.*, **7**, E61–E77.

2. Liu,M.A. (2003) DNA vaccines: a review. *J. Int. Med.*, **253**, 402–410.
3. Kawaguchi,M., Yamazaki,J., Ohno,J. and Fukushima,T. (2012) Preparation and binding study of a complex made of DNA-treated single-walled carbon nanotubes and antibody for specific delivery of a 'molecular heater' platform. *Int. J. Nanomed.*, **7**, 4363–4371.
4. Umemura,K. (2015) Hybrids of nucleic acids and carbon nanotubes for nanobiotechnology. *Nanomat*, **5**, 321–350.
5. Goldman,N., Bertone,P., Chen,S., Dessimoz,C., LeProust,E.M., Sipos,B. and Birney,E. (2013) Towards practical, high-capacity, low-maintenance information storage in synthesized DNA. *Nature*, **494**, 77–80.
6. Pogozelski,W.K. and Tullius,T.D. (1998) Oxidative strand scission of nucleic acids: Routes initiated by hydrogen abstraction from the sugar moiety. *Chem. Rev.*, **98**, 1089–1108.
7. Cadet,J., Delatour,T., Douki,T., Gasparutto,D., Pouget,J.P., Ravanat,J.L. and Sauvaigo,S. (1999) Hydroxyl radicals and DNA base damage. *Mutat. Res./Fundam. Mol. Mech. Mutagen.*, **424**, 9–21.
8. Bonnet,J., Colotte,M., Coudy,D., Couallier,V., Portier,J., Morin,B. and Tuffet,S. (2010) Chain and conformation stability of solid-state DNA: Implications for room temperature storage. *Nucleic Acids Res.*, **38**, 1531–1546.
9. Paunescu,D., Fuhrer,R. and Grass,R.N. (2013) Protection and deprotection of DNA: High-temperature stability of nucleic acid barcodes for polymer labeling. *Angew. Chem. Int. Ed.*, **52**, 4269–4272.
10. Lou,J.J., Mirsadraei,L., Sanchez,D.E., Wilson,R.W., Shabihkhani,M., Lucey,G.M., Wei,B., Singer,E.J., Mareninov,S. and Yong,W.H. (2014) A review of room temperature storage of biospecimen tissue and nucleic acids for anatomic pathology laboratories and biorepositories. *Clin. Biochem.*, **47**, 267–273.
11. Ivanov,V.I. and Krylov,D.Y. (1992) A-DNA in solution as studied by diverse approaches. *Methods Enzymol.*, **211**, 111–127.
12. Ivanov,V.I., Minchenkova,L.E., Minyat,E.E., Frank-Kamenetskii,M.D. and Schyolkina,A.K. (1974) The B to A transition of DNA in solution. *J. Mol. Biol.*, **87**, 817–833.
13. Swatloski,R.P., Spear,S.K., Holbrey,J.D. and Rogers,R.D. (2002) Dissolution of cellulose with ionic liquids. *J. Am. Chem. Soc.*, **124**, 4974–4975.
14. Ghoshdastidar,D., Ghosh,D. and Senapati,S. (2016) High nucleobase-solubilizing ability of low-viscous ionic liquid/water mixtures. *J. Phys. Chem. B*, **120**, 492–503.
15. Vijayaraghavan,R., Izgorodin,A., Ganesh,V., Surianarayanan,M. and MacFarlane,D.R. (2010) Long-term structural and chemical stability of DNA in hydrated ionic liquids. *Angew. Chem. Int. Ed.*, **49**, 1631–1633.
16. Chandran,A., Ghoshdastidar,D. and Senapati,S. (2012) Groove binding mechanism of ionic liquids: a key factor in long-term stability of DNA in hydrated ionic liquids? *J. Am. Chem. Soc.*, **134**, 20330–20339.
17. Malenkov,G., Minchenkova,L., Minyat,E., Schyolkina,A. and Ivanov,V. (1975) The nature of the B-A transition of DNA in solution. *FEBS Lett.*, **51**, 38–42.
18. Saenger,W., Hunter,W.N. and Kennerd,O. (1986) DNA conformation is determined by economics in the hydration of phosphate groups. *Nature*, **24**, 385–388.
19. Whelan,D.R., Bambery,K.R., Heraud,P., Tobin,M.J., Diem,M., McNaughton,D. and Wood,B.R. (2011) Monitoring the reversible B to A-like transition of DNA in eukaryotic cells using Fourier transform infrared spectroscopy. *Nucleic Acids Res.*, **39**, 5439–5448.
20. Cheatham,T.E. III and Kollman,P.A. (1996) Observation of the A-DNA to B-DNA transition during unrestrained molecular dynamics in aqueous solution. *J. Mol. Biol.*, **259**, 434–444.
21. Jayaram,B., Sprous,D., Young,M.A. and Beveridge,D.L. (1998) Free energy analysis of the conformational preferences of A and B forms of DNA in solution. *J. Am. Chem. Soc.*, **120**, 10629–10633.
22. Mazur,A.K. (2003) Titration *in silico* of reversible B ↔ A transitions in DNA. *J. Am. Chem. Soc.*, **125**, 7849–7859.
23. Pastor,N. (2005) The B- to A-DNA transition and the reorganization of solvent at the DNA surface. *Biophys. J.*, **88**, 3262–3275.
24. Case,D.A. (2012) *AMBER 12*. University of California, San Francisco.
25. Chandran,A., Prakash,K. and Senapati,S. (2010) Structure and dynamics of acetate anion-based ionic liquids from molecular dynamics study. *Chem. Phys.*, **374**, 46–54.
26. Cheatham,T.E. III, Crowley,M.F., Fox,T. and Kollman,P.A. (1997) A molecular level picture of the stabilization of A-DNA in mixed ethanol–water solutions. *Proc. Natl. Acad. Sci. U.S.A.*, **94**, 9626–9630.
27. Sprous,D., Young,M.A. and Beveridge,D.L. (1998) Molecular dynamics studies of the conformational preferences of a DNA double helix in water and an ethanol/water mixture. *J. Phys. Chem. B*, **102**, 4658–4667.
28. Knee,K.M., Dixit,S.B., Aitken,C.E., Ponomarev,S., Beveridge,D.L. and Mukerji,I. (2008) Spectroscopic and molecular dynamics evidence for a sequential mechanism for the A-to-B transition in DNA. *Biophys. J.*, **95**, 257–272.
29. Sarai,A., Jernigan,R.L. and Mazur,J. (1996) Interdependence of conformational variables in double-helical DNA. *Biophys. J.*, **71**, 1507–1518.
30. Lavery,R., Maddocks,J.H., Pasi,M. and Zakrzewska,K. (2014) Analyzing ion distributions around DNA. *Nucleic Acids Res.*, **42**, 8138–8149.
31. Dickerson,R.E. (1992) DNA structure from A to Z. *Methods Enzymol.*, **211**, 67–111.